リポソームとリポプレックスの物性測定

リポソームとリポプレックスのサイズと表面電位は、電気泳動光散乱光度計（ELS-Z2、大塚電子（株））を用いて、表面の水和状態は蛍光物質6-dodecanoyl-2-dimethylaminonaphthalene (laurdan)を0.2mol%総脂質に対して添加したリポソームを用いて、25℃でEx340nmおけるEm440と490 nmでの蛍光強度の差からGP (generalized polarization) 値を求めて評価した。

$$GP = (I_{440} - I_{490})/(I_{440} + I_{490})$$

誘電率と誘電緩和は、デジタイジングオシロスコープ(54120B 型、アジレント製)によって、25℃水中で総脂質濃度 11.2 mg/mL のリポソームを用いて行った。コントロールとして pDNA 水溶液の測定を行い、リポプレックスの測定値から差し引いた。

C．研究結果

リポソームの PEG 脂質による表面修飾と表面電位、水和状態との関係を調べた。

各リポソームにおいては、PEG 修飾率が高くなると表面電位は低下する傾向が見られた。

蛍光標識したリポソームの蛍光強度から導き出される GP 値は水和状態の指標とされており、この値が高いほど脱水和状態にあるとされている。PEG 脂質で１～10%修飾した OH-Chol リポソームにおいては、１%と 5%で GP 値が低下した(Fig. 2A、B)。DOTAP / DOPE / DSPE-PEG リポソームでは、GP 値が OH-Chol リポソームより全体に低くなった(Fig. 2C)。これは、DOTAP / DOPE のリポソームの 4 級アミンが水和しやすいためと考えられる。

OH-Chol リポソームの GP 値を超純水と PBS 中で測定したとき、PBS 中のほうが水中より GP 値は高くなった。これは PBS 中に含まれるイオンが正電荷脂質に対して脱水和作用を引き起こしたためと考えられる（Fig. 3）。

次に、このリポソームおよびリポプレックスの GP 測定を行った（Fig. 4）。リポプレックスは荷電比＋/－＝3/1 となるように調製した。PEG 未修飾では DNA との混合直後に凝集が観察されたため、調製できた 1.0%、1.5%、5%PEG 修飾のリポプレックスにおいて GP 値の測定を行った。リポソームとリポプレックスの GP 値を比較すると、リポプレックスの GP 値のほうが高くなり、脱水和することがわかった。

このリポソームおよびリポプレックスの誘電緩和時間測定を行ったところ、PEG 修飾リポソームとリポプレックスにおいては、PEG 修飾量が増加するとともに緩和時間の減少が見られ、脱水和する傾向が観察された（Fig. 5）。これは、Fig. 4 より PBS 中で測定した GP 値から、5%PEG 修飾リポプレックスは脱水和しているという結果と一致した。

D．考察

遺伝子導入用リポソームベクターでは、一般にカチオン性脂質が用いられている。アニオン性の pDNA とリポプレックスを作り、なおかつアニオン性電荷をもつ細胞と相互作用させるために、カチオン性リポソームと pDNA の(+/-)荷電比を調整してカチオン性にしている。従って、このカチオン性脂質のリポプレックスにおいては、pDNA とリポソーム脂質膜との強い静電的相互作用により、サイズや表面状態が変化することが知られている。そのため、これまではリポプレックスの表面状態は表面電位で評価されてきた。ここでは表面の水和状態を新たな方法で測定することにより、細胞内取り込みに最適なカチオン性リポソームと pDNA の混合比を決定できる可能性を検討した。

まず、カチオン性脂質としては、生体分解性が高く、pDNA と適度に相互作用をする脂質として、コレステロール誘導体（OH-Chol）を選択した。リポソームの表面電位は、PEG 脂質の添加によっ

て低下する傾向を示した。これは、OH-Chol の二級アミノ基の解離状態が PEG によって遮蔽されるためと推察された。また、GP 値からみたリポソームの水和状態は、PEG 修飾の増加によって水和する傾向を示し、リポプレックスでは脱水和する傾向を示した。

誘電緩和時間測定からも、PEG 修飾リポソームにおいて、PEG 修飾が増加すると水和し、そのリポプレックスにおいては脱水和する傾向がみられた。GP 値は蛍光物質の分布するカチオン性脂質の極性基近傍の水和状態を反映している。誘電緩和時間は溶液中の水分子の平均の動きを反映しており、カチオン性脂質の極性基に水和した水分子と PEG 鎖に水和した水分子も緩和時間の増加に寄与していると推察される。したがって、リポソーム全体の水和状態を反映すると考えられる。

E．結論

本研究の結果より、誘電緩和時間は、PEG 修飾リポソームとリポソーム/pDNA 複合体のカチオン性の極性基と PEG 鎖長の全体の水和状態を示すパラメーターとなることが示唆された。この測定法は、PEG 修飾リポソームの表面水和状態の解明に有用となる可能性が示唆された。

F．健康危険情報

なし

G．研究発表

1. 論文発表

1) Kawano, Y. Maitani, Tumor permeability of nanocarriers observed by dynamic contrast-enhanced magnetic resonance imaging, *Yakugaku Zasshi*, **130** (12), 1679-1685 (2010).

2) K. Shiraishi, K. Kawano, Y. Maitani, Yokoyama M. Polyion complex micelle MRI contrast agents from poly(ethylene glycol)-b-poly(L-lysine) block copolymers having Gd-DOTA; preparations and their control of T_1-relaxivities and blood circulation characteristics. J Control Release, 148, 160-167 (2010).

3) Y. Hattori, N. Kanamoto, K. Kawano, H. Iwakura, M. Sone, M.Miura, A. Yasoda, N. Tamura, H. Arai, T. Akamizu, K. Nakao, Y. Maitani, Molecular characterization of tumors from a transgenic mice adrenal tumor model: Comparison with human pheochromocytoma, International Journal of Oncology, 37:695-705 (2010).

4) Y. Taniguchi, K. Kawano, T. Minowa, T. Sugino, Y. Shimojo, Y. Maitani, Enhanced Antitumor Efficacy of Folate-linked Liposomal Doxorubicin with TGF-ß Type I Receptor Inhibitor, Cancer Science, 101, 2207-2213 (2010).

5) A. Hioki , A. Wakasugi, K. Kawano, Y. Hattori, Y. Maitani, Development of an In Vitro Drug Release Assay of PEGylated Liposome Using Bovine Serum Albumin and High Temperature, Biol. Pharm. Bull., 33, 1466-1470 (2010).

6) Y. Maitani, Lipoplex formation using liposomes prepared by ethanol injection. Methods Mol Biol.605: 393-403 (2010).

7) Y. Hattori, M. Hakoshima, K. Koga and Y. Maitani, Increase of therapeutic effect by treating nasopharyngeal tumor with combination of HER-2 siRNA and paclitaxel, International Journal of Oncology, 36: 1039-1046 (2010).

8) K. Koga , Y. Hattori, M. Komori, R. Narishima, M. Yamasaki, M. Hakoshima, T. Fukui and Y. Maitani, Combination of RET siRNA and irinotecan inhibited the growth of medullary thyroid carcinoma TT cells and xenografts *via* apoptosis, Cancer Science, 101: 941-947 (2010).

9) H. Ma, K. Shiraishi, T. Minowa, K. Kawano, M. Yokoyama, Y. Hattori, Y. Maitani, Accelerated blood clearance was not induced for a gadolinium-containing PEG-poly(L-lysine)-based polymeric micelle in mice, Pharm Res, 27(2):296-302 (2010).

2. 学会発表

1. 若杉亜以, 浅川真澄, 小木曽真樹, 清水敏美, 米谷芳枝 オーガニックナノチューブを用いた新規ドラッグデリバリーシステムの構築

SORST シンポジウム(4) (2010. 1)

2. 服部喜之, 金本巨哲, 川野久美, 岩倉浩, 赤水尚史, 中尾一和, 米谷芳枝 副腎腫瘍自然発症遺伝子改変マウスの DNA マイクロアレイによる遺伝子解析 第 83 回日本内分泌学会(2010.3)

3. 川野久美, 服部喜之, 岩倉浩, 赤水尚史, 米谷芳枝 副腎腫瘍発症遺伝子改変マウスに対する抗癌剤微粒子製剤と分子標的薬の併用治療効果 第 83 回日本内分泌学会(2010.3)

4. 川野久美, 米谷芳枝 DCE-MRI を用いた TGF-β 阻害剤併用時の微粒子製剤の腫瘍移行性評価 日本薬学会 第 130 年会(2010.3)

5. 泉澤友宏, 服部喜之, 戸澗一孔 米谷芳枝 プロテオグリカンを介したデカアルギニン脂質/DNA 複合体の細胞内取り込み 日本薬学会 第 130 年会(2010.3)

6. 岩瀬由布子, 米谷芳枝 オクトレオチド修飾リポソーム製剤の調製と *in vitro* 評価日本薬学会 第 130 年会(2010.3)

7. 若杉亜以, 浅川真澄, 小木曽真樹, 清水敏美, 米谷芳枝 オーガニックナノチューブの薬物キャリアーへの応用日本薬学会 第 130 年会(2010.3)

8. 尾上裕貴, 林京子, 李貞範, 米谷芳枝, 甲斐敬, 林利光 単純ヘルペスウイルス感染症治療におけるポリエチレンイミンの特性日本薬学会 第 130 年会(2010.3)

9. 生形晴哉, 服部喜之, 米谷芳枝 アンギオテンシンIIによる昇圧下でのリポソーム製剤の腫瘍集積性の検討日本薬学会 第 130 年会(2010.3)

10. 勢子祐貴, 服部喜之, 米谷芳枝 スニチニブ封入リポソーム製剤のラット副腎髄質褐色細胞腫担癌ヌードマウスに対する評価 日本薬学会 第 130 年会(2010.3)

11. 中野宏樹, 置田裕子, 石井佑太, 長岡康夫、上里新一, 服部喜之, 米谷芳枝 新規遺伝子発現増強剤 DDTS-K-182 日本薬学会 第 130 年会(2010.3)

12. Kanamoto, N., Takeuchi, Y., Hattori, Y., Yoshida, M., Kondo, E., Yamada, G., Fujii, T., Saijo, M., Nambu, T., Miura, M., Yasoda, A., Arai, H., Maitani, Y. and Nakao, K. Expression of folate receptor type α gene in thyroid papillary carcinoma 第 14 回国際内分泌学会 (2010.3)

13. 中村太郎, 川野久美, 白石貢一, 横山昌幸, 米谷芳枝 腫瘍ターゲティング脂質微粒子 MRI 造影剤の調製と評価 第 5 回日本分子イメージング学会(2010.5)

14. 白石貢一, 川野久美, 米谷芳枝, 横山昌幸 高分子ミセル MRI 造影剤と ABC 現象の検証 第 5 回日本分子イメージング学会(2010.5)

15. 田中拓海, 阿曽幸男, 米谷芳枝 リポソームの表面水和状態と細胞内取り込み 日本薬剤学会 第 25 年会 (2010.5)

16. 田中拓海, 服部喜之, 米谷芳枝 アンギオテンシンII昇圧下における正電荷リポソームの癌遺伝子送達 第 26 回日本 DDS 学会 (2010.6)

17. 加藤真子, 服部喜之, 米谷芳枝 静脈内投与したリポプレックスの腫瘍集積性に及ぼす

コラゲナーゼ処理の影響 第 26 回日本 DDS 学会 (2010. 6)

18. 坪田結香，川野久美，米谷芳枝 血中滞留性リポソームの腫瘍集積性に対する VEGF 受容体阻害剤の併用効果 第 26 回日本 DDS 学会 (2010. 6)

19. 荒金大介，中澤裕太，泉澤友宏，宮下久徳，石垣賢二，林京子，甲斐敬，米谷芳枝 抗ウイルス剤ポリエチレンイミン(PEI)の弱毒化を目的としたリポソーム及びキトサンの併用効果 第 26 回日本 DDS 学会 (2010. 6)

20. 白石貢一，馬会利，川野久美，米谷芳枝，横山昌幸 高分子ミセル MRI 造影剤の頻回投与による ABC 現象への影響と診断への有用性 第 26 回日本 DDS 学会 (2010. 6)

21. 白石貢一，馬会利，川野久美，米谷芳枝，横山昌幸 高分子ミセルキャリア内核の影響による ABC 現象の発現と回避性 第 26 回日本 DDS 学会 (2010. 6)

22. 渡辺 和男，金子 洵，米谷 芳枝 葉酸修飾ポリ-L-リシンコートリポソームの調製と細胞への取り込み評価 第 26 回日本 DDS 学会 (2010. 6)

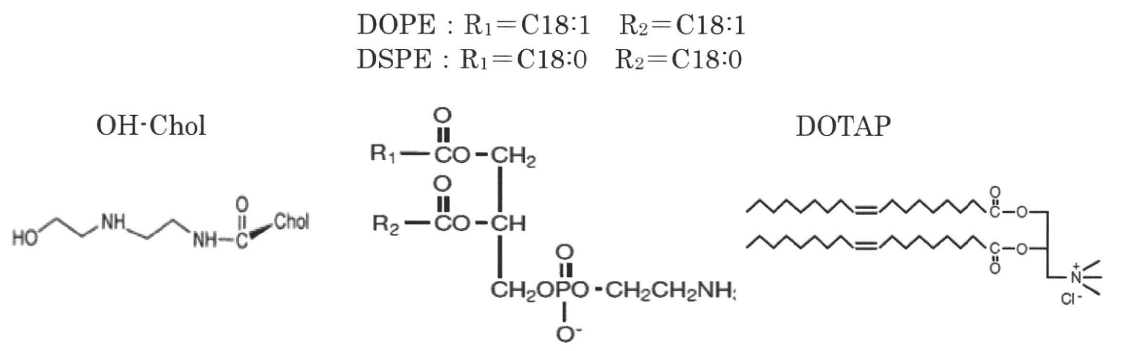

Fig. 1 Chemical structures of lipids

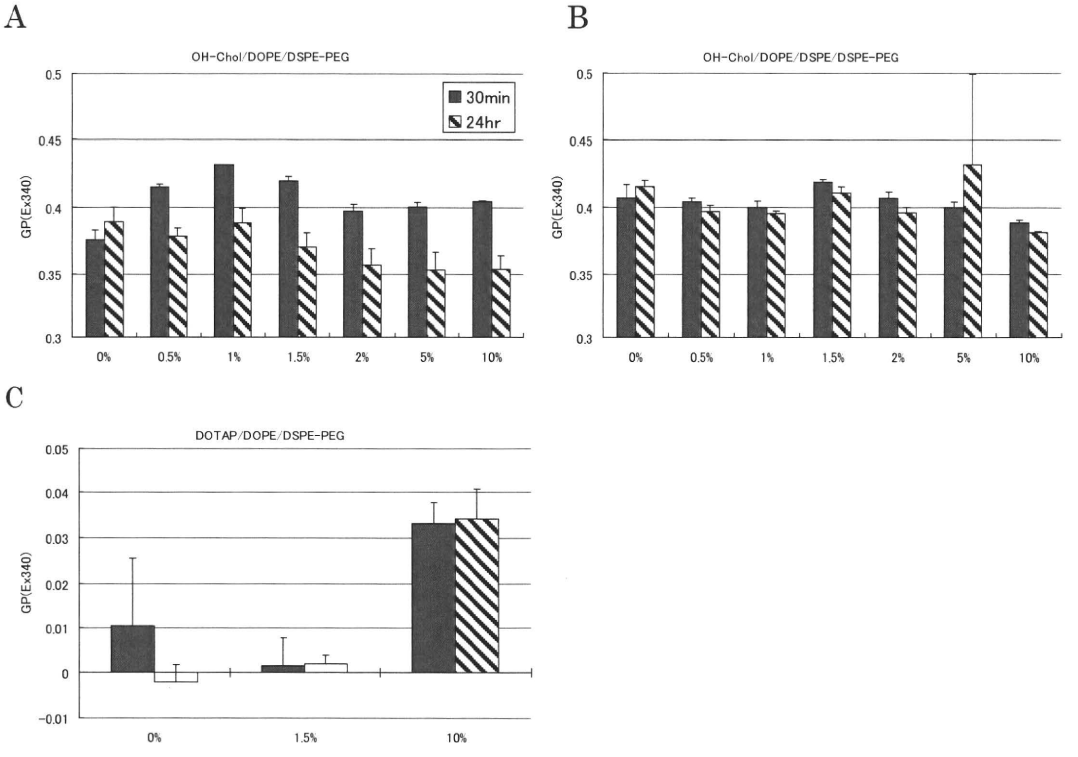

Fig. 2 The change of surface hydration of various PEGylated liposomes as monitored by laurdan generalized polarization(GP) 30 min and 24 hr after dilution with PBS

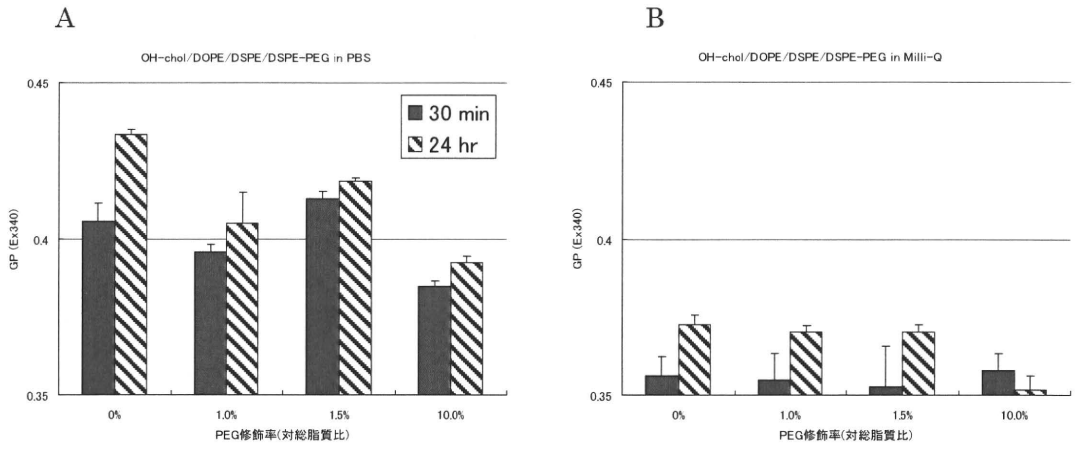

Fig. 3 The change of surface hydration of OH-Chol:DOPE:DSPE:DSPE-PEG_{2000} liposomes as monitored by laurdan generalized polarization(GP) 30 min and 24 hr after dilution with PBS (A) or Milli-Q water (B)

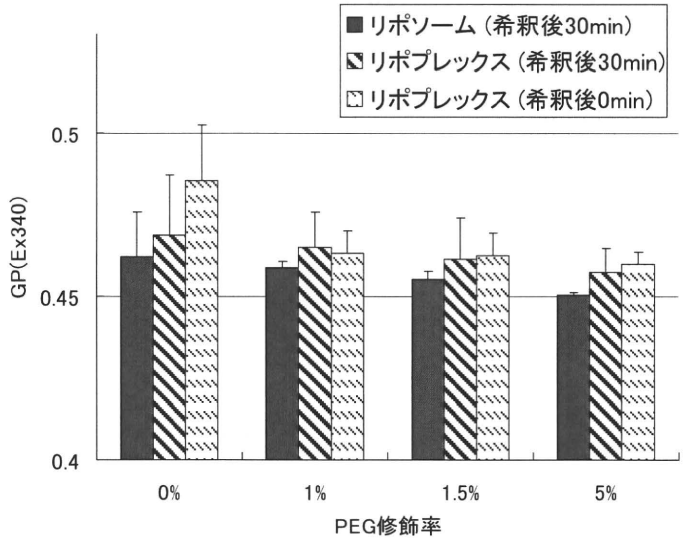

Fig. 4 The change of surface hydration of OH-Chol:DOPE:DSPE:DSPE-PEG_{2000} liposomes and their lipoplexes as monitored by laurdan generalized polarization(GP) 0 min or 30 min after dilution with PBS

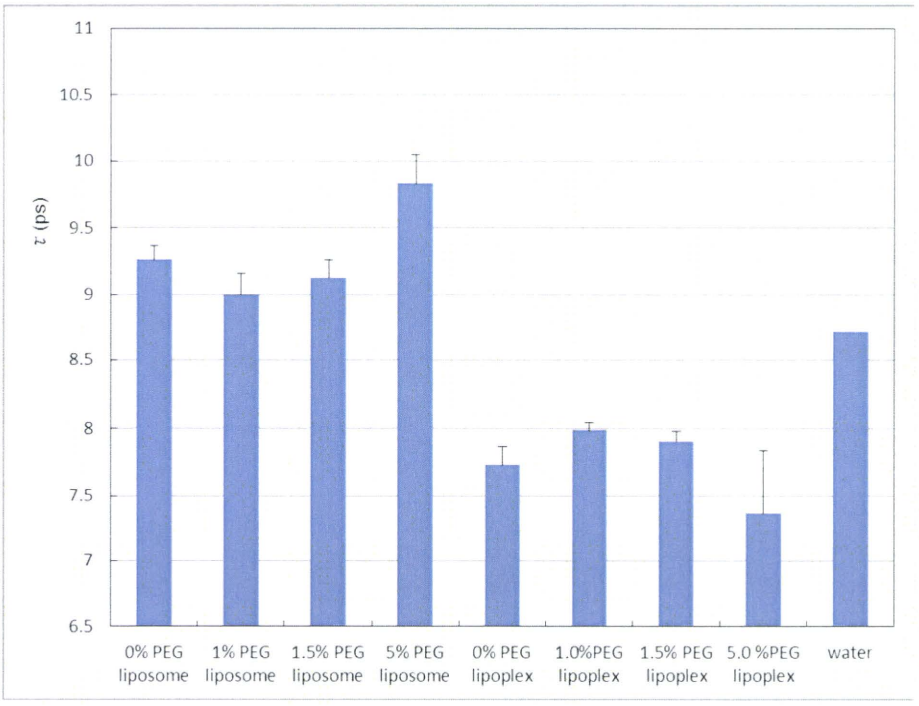

Fig. 5 Dielectric relaxation of OH-Chol:DOPE:DSPE:DSPE-PEG_{2000} liposomes and their lipoplexes in Milli-Q water

別添５

研究成果の刊行に関する一覧表

書籍

著者氏名	論文タイトル	書籍全体の編集者名	書籍名	出版社名	出版地	出版年	ページ
Yoshioka, S., Aso Y.	Molecular Mobility of Freeze-Dried Formulation as Determined by NMR Relaxation times, and Its Effects on Storage Stability.	Rey, L., May, J.C.	Freeze Drying/ Lyophilization of Pharmaceutical and Biological Products,	Informa Healthcare	London	2010	354-371

雑誌

発表者氏名	論文タイトル	発表誌名	巻号	ページ	出版年
Sumie Yoshioka, Kelly M. Forney, Yukio Aso, Michael J. Pikal	Effect of Sugars on the Molecular Motion of Freeze-dried Protein Formulations Reflected by NMR Relaxation Times.	*Pharm. Res.*			accepted
Tamaki Miyazaki, Yukio Aso and Toru Kawanishi	Feasibility of atomic force microscopy for determining crystal growth rates of nifedipine at the surface of amorphous solids with and without polymers.	*J. Pharm. Sci.*			accepted
Tamaki Miyazaki, Yukio Aso, Sumie Yoshioka and Toru Kawanishi	Differences in crystallization rate of nitrendipine enantiomers in amorphous solid dispersions with HPMC and HPMCP.	*Int. J. Pharmaceutics*	407	111-118	2011

Bingquan Wang, Marcus T. Cicerone, Yukio Aso, Michael J. Pikal	The impact of thermal treatment on the stability of freeze-dried amorphous pharmaceuticals: II. aggregation in an IgG1 fusion protein.	*J. Pharm. Sci.*	**99**(2)	683-700	2010
Kawano, Y. Maitani	Tumor permeability of nanocarriers observed by dynamic contrast-enhanced magnetic resonance imaging.	*Yakugaku Zasshi*	**130**(12)	1679-1685	2010
K. Shiraishi, K. Kawano, Y. Maitani, Yokoyama M.	Polyion complex micelle MRI contrast agents from poly(ethylene glycol)-β-poly(l-lysine) block copolymers having Gd-DOTA; preparations and their control of T(1)-relaxivities and blood circulation characteristics.	*J Control Release*	**148**	160-167	2010
Y. Hattori, N. Kanamoto, K. Kawano, H. Iwakura, M. Sone, M.Miura, A. Yasoda, N. Tamura, H. Arai, T. Akamizu, K. Nakao, Y. Maitani	Molecular characterization of tumors from a transgenic mice adrenal tumor model: Comparison with human pheochromocytoma.	*International Journal of Oncology*	**37**	695-705	2010
Y. Taniguchi, K. Kawano, T. Minowa, T. Sugino, Y. Shimojo, Y. Maitani	Enhanced Antitumor Efficacy of Folate-linked Liposomal Doxorubicin with TGF-ß Type I Receptor Inhibitor.	*Cancer Science*	**101**	2207-2213	2010
A. Hioki, A. Wakasugi, K. Kawano, Y. Hattori, Y.	Development of an In Vitro Drug Release Assay	*Biol. Pharm.*	**33**	1466-1470	2010

Maitani	of PEGylated Liposome Using Bovine Serum Albumin and High Temperature.	*Bull*			
Y. Maitani	Lipoplex formation using liposomes prepared by ethanol injection.	*Methods Mol Biol*	**605**	393-403	2010
Y. Hattori, M. Hakoshima, K. Koga and Y. Maitani	Increase of therapeutic effect by treating nasopharyngeal tumor with combination of HER-2 siRNA and paclitaxel.	*International Journal of Oncology*	**36**	1039-1046	2010
K. Koga , Y. Hattori, M. Komori, R. Narishima, M. Yamasaki, M. Hakoshima, T. Fukui and Y. Maitani	Combination of RET siRNA and irinotecan inhibited the growth of medullary thyroid carcinoma TT cells and xenografts via apoptosis.	*Cancer Science*	**101**	941-947	2010
H. Ma, K. Shiraishi, T. Minowa, K. Kawano, M. Yokoyama, Y. Hattori, Y. Maitani	Accelerated blood clearance was not induced for a gadolinium-containing PEG-poly(L-lysine)-based polymeric micelle in mice.	*Pharm. Res.*	27(2)	296-302	2010

研究成果の刊行物・別刷

13 Molecular Mobility of Freeze-Dried Formulations as Determined by NMR Relaxation Times, and Its Effect on Storage Stability

Sumie Yoshioka
University of Connecticut, Storrs, Connecticut, U.S.A.

Yukio Aso
National Institute of Health Sciences, Tokyo, Japan

INTRODUCTION

Freeze-drying is a useful method for preparing dosage forms of thermally unstable pharmaceuticals without the deleterious effect of heat. The method can also provide a dry product of pharmaceuticals with longer shelf life than solutions or suspensions. Although glassy-state formulations obtained by freeze-drying generally exhibit sufficient storage stability for pharmaceuticals, degradation during storage has been observed in various freeze-dried formulations.

Many studies have demonstrated that storage stability of freeze-dried formulations is related to molecular mobility (1–15). Chemical and physical degradation of small molecules and proteins is enhanced by an increase in molecular mobility associated with moisture sorption. Additives that decrease the molecular mobility of formulations are often effective for the stabilization of the formulation.

This chapter describes molecular mobility of freeze-dried formulations as determined by NMR relaxation times and discusses the relationship between storage stability and NMR-determined molecular mobility.

MOLECULAR MOBILITY AS DETERMINED BY NMR RELAXATION TIMES

NMR has been used to determine molecular mobility of freeze-dried formulations (16–20), along with other techniques like calorimetry, dielectric relaxation spectrometry, and dynamic mechanical measurement (21–25). NMR can determine the mobility of atoms in pharmaceutical molecules such as ^{1}H, ^{2}H, ^{13}C, ^{15}N, ^{17}O, and ^{19}F. To determine the mobility of a specific site in the molecule, high-resolution solid-state NMR with high sensitivity is necessary. Especially, high sensitivity is inevitable for ^{13}C and ^{15}N, which have low natural abundance. In contrast, low-frequency solid-state NMR, which is easier to operate than high-resolution NMR, can be used to determine the mobility of ^{1}H and ^{19}F, which have high natural abundance. This section addresses the molecular mobility of ^{1}H, ^{13}C, and ^{19}F measured by each of low-frequency solid-state NMR and high-resolution solid-state NMR.

Molecular Mobility as Determined by Low-Frequency NMR

Spin-Spin Relaxation Time of Proton

Spin-spin relaxation time (T_2) of protons present in freeze-dried formulations can be determined from free induction decay (FID). Figure 1 shows the FID of

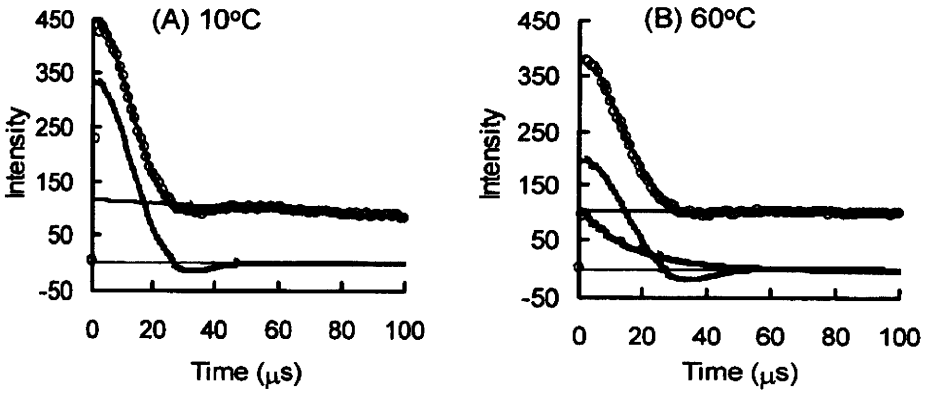

FIGURE 1 Free induction decay of proton in freeze-dried γ-globulin formulation containing dextran at 10°C (**A**) and 60°C (**B**) at 60% RH. *Abbreviation*: RH, relative humidity.

proton in freeze-dried formulation containing γ-globulin as a model protein drug and dextran (molecular weight of 10 kDa) as a polymer excipient, measured by a low-frequency NMR using "solid echo" in the detection stage (26). The FID shows two relaxation processes at 10°C and 60% relative humidity (RH) (Fig. 1A); a slower decay described by the Lorentzian equation (equation 1) and a faster decay described by a Gaussian-type equation (the Abragam equation, equation 2 with a constant c of 0.12). This slower decay is attributed to protons with higher mobility, that is, water protons, and the faster decay is attributed to protons with lower mobility, that is, protons of γ-globulin and dextran. The contribution of protein protons to the FID is not significant because the content of protein was 50 times less than that of dextran. Therefore, the Abragam decay can be considered to be due to dextran protons. The observed FID is describable by an equation representing the sum of the Abragam and Lorentzian equations (equation 3). The T_2 of water protons can be calculated from the FID signals at the latter stage. Subsequently, the T_2 of dextran proton with lower mobility can be calculated from the FID signals at the former stage by inserting the calculated T_2 of water proton into equation (3).

$$F(t) = A\exp\left(-\frac{t}{T_{2(\mathrm{hm})}}\right) \tag{1}$$

$$F(t) = A\exp\left(-\frac{t^2}{2T_{2(\mathrm{lm})}{}^2}\right)\frac{\sin(ct)}{ct} \tag{2}$$

$$F(t) = (1 - P_{\mathrm{hm}})\exp\left(-\frac{t^2}{2T_{2(\mathrm{lm})}{}^2}\right)\frac{\sin(ct)}{ct} + P_{\mathrm{hm}}\exp\left(-\frac{t}{T_{2(\mathrm{hm})}}\right) \tag{3}$$

where $T_{2(\mathrm{hm})}$ and $T_{2(\mathrm{lm})}$ are the spin-spin relaxation times of protons with higher mobility and lower mobility, respectively. P_{hm} is the proportion of protons with higher mobility.

As shown in Figure 1B, the decay due to dextran protons at 60°C cannot be described by a single Abragam equation, and therefore requires further solving by the Lorentzian equation. This indicates that at 60°C, the dextran protons in the freeze-dried formulation exhibit a slower relaxation process due to higher mobility in addition to a faster relaxation process due to lower mobility. In other words, dextran protons having higher mobility exist in the formulation at 60°C, in addition to solid-like dextran protons with lower mobility. Thus, the FID at 60°C is described by an equation representing the sum of the Abragam and Lorentzian equations for dextran protons as well as the Lorentzian equation for water protons. The proportion of dextran protons having higher mobility can be calculated by fitting FID signals into equation (3) after subtracting signals due to water protons.

The temperature at which the spin-spin relaxation of proton begins to involve the Lorentzian relaxation process due to polymer protons having higher mobility in addition to the Gaussian-type relaxation process due to polymer protons having low mobility is considered to be a glass/rubber transition temperature. Basically, this is a critical temperature of molecular mobility as determined by NMR relaxation measurements and is analogous to glass transition temperature (T_g) determined by differential scanning calorimetry (DSC). This critical mobility temperature is referred to as T_{mc}. The T_{mc} of formulations containing polymer excipients increases as the molecular weight of the polymers increases. The T_{mc} of a formulation containing dextran with a molecular weight of 510 kDa is 5°C higher than that for dextran with a molecular weight of 40 kDa. Similarly, the T_{mc} of molecular weight 120 kDa poly(vinyl alcohol) (PVA) formulation is approximately 5°C higher than that of molecular weight 18 kDa PVA formulation (27). In contrast, the T_2 of water proton calculated by the Lorentzian equation is not significantly affected by the molecular weight of dextran (26). This indicates that the mobility of water molecules in the formulation is determined by the interaction between the glucose unit and water.

Figure 2 shows the effect of water content on the T_{mc} and T_g of freeze-dried γ-globulin formulations containing dextran, polyvinylpyrrolidone (PVP) and α,β-poly(*N*-hydroxyethyl)-L-aspartamide (PHEA) (28). T_{mc} shifts to a lower temperature as water content increases, indicating that the molecular

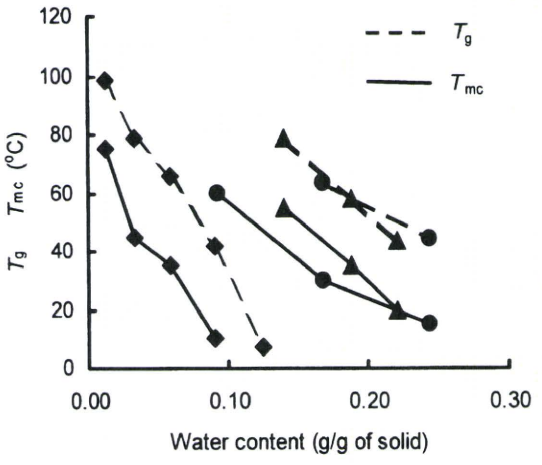

FIGURE 2 T_{mc} and glass transition temperature of freeze-dried γ-globulin formulations containing PHEA (■), dextran (▲), and PVP (●). *Abbreviations*: PHEA, α,β-poly(*N*-hydroxyethyl)-L-aspartamide; PVP, polyvinylpyrrolidone.

mobility of polymer excipients in the formulation is increased by the plasticizing effect of water. Decrease in T_{mc} with increasing water content is also observed for other freeze-dried formulations containing PVA, methylcellulose (MC), hydroxypropylmethylcellulose, and carboxymethylcellulose sodium salt.

The T_{mc} of freeze-dried formulations containing polymer excipients is generally observed at a temperature of 20°C to 30°C lower than the T_g determined by DSC (Fig. 2). This indicates that these formulations have highly mobile protons even at temperatures below the T_g. T_{mc} can be considered to be the temperature at which a certain region of the molecule, such as terminal units of polymer chains, begins to have greater mobility. T_{mc} is a glass/rubber transition temperature determined by spin-spin relaxation measurements, which can detect local changes in molecular mobility more sensitively than T_g determined by DSC. The T_g of freeze-dried formulations containing polymer excipients with moisture is often difficult to determine because a change in heat capacity at T_g may be overlapped by the peaks of water evaporation and accompanying relaxation processes. Furthermore, certain formulations, especially freeze-dried protein formulations, reveal unclear changes in heat capacity, causing a difficulty in determination of T_g. In such cases, T_{mc} determined by spin-spin relaxation measurement can be a useful measure of T_g.

Laboratory and Rotating Frame Spin-Lattice Relaxation Times of Proton

Along with T_2, spin-lattice relaxation times in laboratory and rotating frames (T_1 and $T_{1\rho}$) can also be used to measure the molecular mobility of freeze-dried formulations. The T_1 and $T_{1\rho}$ of proton reflect the correlation time (τ_c) of the rotational motion of proton. The relationship between τ_c and T_1 can be described as follows:

$$\frac{1}{T_1} = \frac{3}{10}\gamma^4\left(\frac{h}{2\pi}\right)^2 r^{-6}\left(\frac{\tau_c}{1+\omega_0^2\tau_c^2} + \frac{4\tau_c}{1+4\omega_0^2\tau_c^2}\right) \tag{4}$$

where γ is the gyromagnetic ratio of ^1H, h is Planck's constant, ω_0 is the ^1H resonance frequencies, and r is the H-H distance. In contrast, $T_{1\rho}$ can be related to τ_c according to equation (5).

$$\frac{1}{T_{1\rho}} = \frac{A\tau_c}{1+4\omega_1^2\tau_c^2} \tag{5}$$

where ω_1 is the frequency of precession generated by the spin locking field and A is a constant.

Figure 3 shows the relationship between τ_c and T_1 (or $T_{1\rho}$) of proton. When τ_c exhibits an Arrhenius behavior, T_1 (or $T_{1\rho}$) exhibits a similar V-shaped pattern with a minimum as a function of temperature. In the temperature range below the minimum (slow motional regime), T_1 (or $T_{1\rho}$) increases in a linear fashion with decreasing temperature (i.e., with decreasing mobility). In the temperature range above the minimum (fast motional regime), in contrast, T_1 (or $T_{1\rho}$) decreases with decreasing mobility associated with decreasing temperature. T_1 minimum is observed at a higher temperature than $T_{1\rho}$ minimum, such that T_1 sensitively reflects faster motion than $T_{1\rho}$ does.

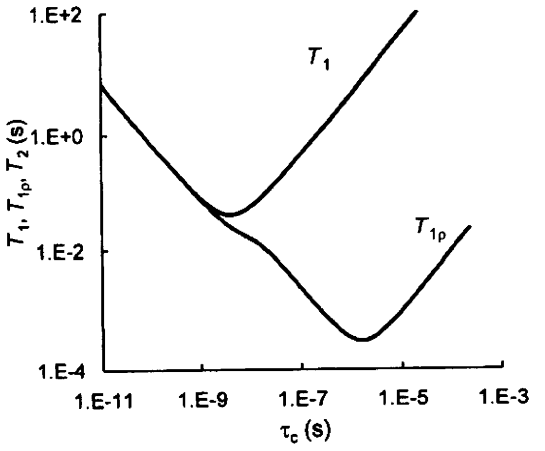

FIGURE 3 Relationship between NMR relaxation times and correlation time.

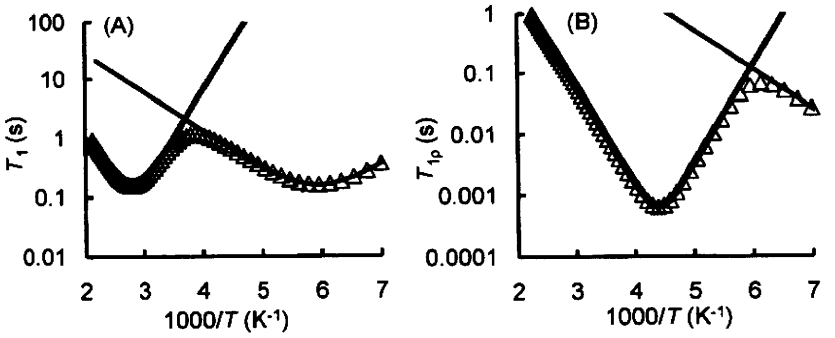

FIGURE 4 Temperature dependence of T_1 **(A)** and $T_{1\rho}$ **(B)** of proton with two correlation times.

When there are multiple protons having different τ_c values in the molecule, spin diffusion occurs between protons located within a short distance, and gives a single T_1 (or $T_{1\rho}$) value. Therefore, the value of T_1 (or $T_{1\rho}$) is determined mainly by a proton that shows the shortest relaxation time. As described by equation (6), relaxation rate (the reciprocal of T_1 and $T_{1\rho}$) can be calculated as the sum of the relaxation rates attributed to each τ_c, when there are two protons having different τ_c values (τ_{c1} and τ_{c2}) in the system. Thus, the observed values of T_1 and $T_{1\rho}$ closely approximate the smaller relaxation times of the two loci, as shown in Figure 4.

$$\frac{1}{T_{1(\text{obs})}} = \frac{P_1}{T_{1(\tau_{c1})}} + \frac{(1-P_1)}{T_{1(\tau_{c2})}} \tag{6}$$

where P_1 is the fraction of proton having τ_{c1}.

Figure 5 shows the temperature dependence of $T_{1\rho}$ observed for freeze-dried γ-globulin formulations containing dextran, prepared using D_2O (29). Since the ratio of γ-globulin to dextran is 1:50, the calculated $T_{1\rho}$ represents the $T_{1\rho}$ of unexchangeable protons of dextran (5 methine protons and 2 methylene protons in a repeating unit). The temperature dependence of $T_{1\rho}$ exhibits a

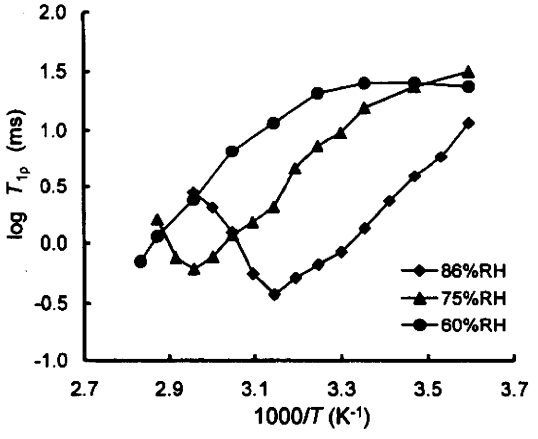

FIGURE 5 Spin-lattice relaxation time of dextran proton in freeze-dried γ-globulin containing dextran.

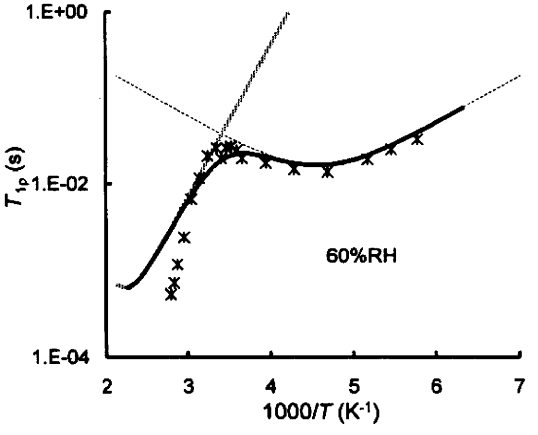

FIGURE 6 Spin-lattice relaxation time of dextran proton in freeze-dried γ-globulin containing dextran in a wider temperature range.

minimum at relatively high humidities (75% and 86% RH). The temperature of the $T_{1\rho}$ minimum shifts to higher temperature as humidity decreases. At 60% RH, minimum is not observed in the temperature range up to 80°C (it may be observed around 90°C), but another minimum is observed at approximately −60°C, as shown in Figure 6. This minimum shifts to approximately 90°C in the dry state. These findings indicate that proton has two different correlation times due to different motions.

The temperature dependence for the $T_{1\rho}$ of proton observed at 60% RH (Fig. 6) can be described by two correlation times (τ_{c1} and τ_{c2}) with an activation energy of 8.0 and 2.5 kcal/mol, and with a pre-exponential factor of 2×10^{-10} and 5×10^{-9}seconds, respectively, at temperatures lower than 35°C (1000/T of 3). The motion represented by τ_{c1} and τ_{c2} may be attributed to methine and methylene protons, respectively, on the basis of the values of activation energy. An activation energy of the same order as the calculated value of τ_{c2} has been reported for the methylene group of amorphous polyethylene (3.72 kcal/mol) (30). $T_{1\rho}$ reflects the motion of methine groups at temperatures between 35°C and 10°C (1000/T of 3 and 3.5), but reflects the motion of methylene groups at

temperatures lower than 10°C. The observed $T_{1\rho}$ of methine groups diverges from the values calculated from τ_{c1} at temperatures above 35°C, indicating that the motion of methine groups has greater activation energy at temperature above 35°C. The temperature at which a break is observed in the temperature dependence is coincident with T_{mc}, described in the section of proton T_2.

Molecular Mobility as Determined by High-Resolution NMR

Laboratory and Rotating Frame Spin-Lattice Relaxation Times of Carbon

Figure 7 shows the typical spectra of freeze-dried γ-globulin formulation containing dextran, freeze-dried γ-globulin, and freeze-dried dextran, measured by high-resolution ^{13}C solid-state NMR (31). Peaks at 70 and 180 ppm are assigned to the dextran methine carbon and γ-globulin carbonyl carbon, respectively. The T_1 of each carbon, calculated from the signal decay, decreases with increasing temperature, indicating that relaxation occurs in the slow motional regime. The τ_c of dextran methine carbon then can be calculated from the observed T_1 according to equation (7), if the dipole-dipole interaction between carbon and proton is predominant in the relaxation process, and if the relaxation time can be expressed by a single τ_c.

$$\frac{1}{T_1} = \frac{1}{10}\gamma_C^2\gamma_H{}^2\left(\frac{h}{2\pi}\right)^2 r_{C-H}{}^{-6} \times \left[\frac{\tau_c}{1+(\omega_c-\omega_H)^2\tau_c{}^2} + \frac{3\tau_c}{1+\omega_c^2\tau_c{}^2} + \frac{6\tau_c}{1+(\omega_C+\omega_H)^2\tau_c{}^2}\right] \quad (7)$$

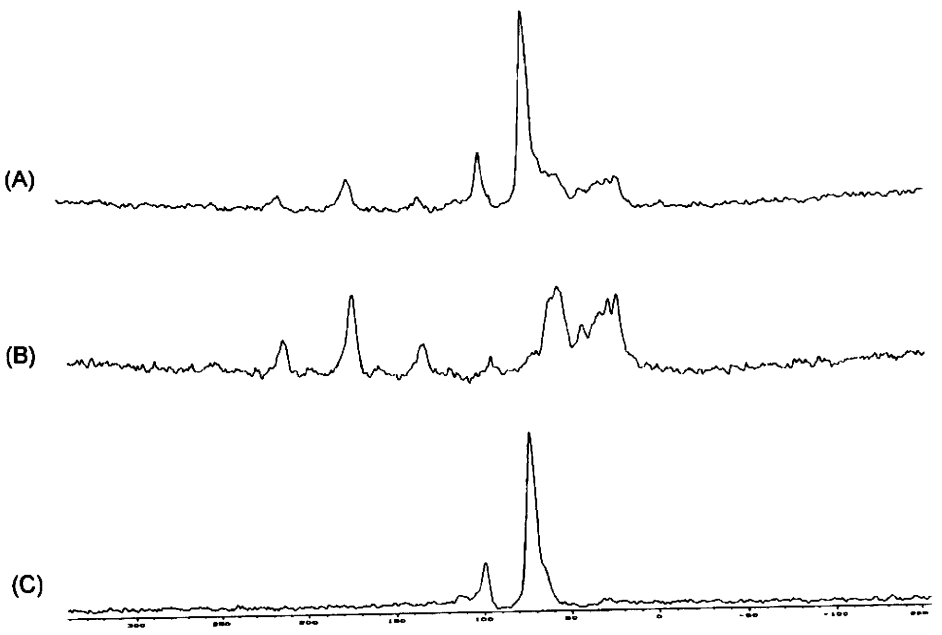

FIGURE 7 ^{13}C-NMR spectra of freeze-dried γ-globulin formulations containing dextran **(A)**, freeze-dried γ-globulin **(B)**, and freeze-dried dextran **(C)**.

where γ_C and γ_H are the gyromagnetic ratios of ^{13}C and ^{1}H, respectively, h is the Planck's constant, and ω_C and ω_H are the ^{13}C and ^{1}H resonance frequencies, respectively. $r_{C\text{-}H}$ is the C-H distance and a value of 1.2Å was used for the calculation.

In contrast, the τ_c of γ-globulin carbonyl carbon can be calculated from the observed T_1 using equation (8) if the relaxation due to chemical shift anisotropy is predominant, and if the relaxation time in the slow motional regime can be expressed by a single τ_c.

$$\frac{1}{T_1} = \frac{6}{40}\gamma_C{}^2 B_0^2 \delta_Z{}^2 \left(1 + \frac{\eta^2}{3}\right)\left(\frac{2\tau_c}{1+\omega_0{}^2\tau_c{}^2}\right) \tag{8}$$

where B_0, δ_Z, and η are the static field, the chemical shift anisotropy, and the asymmetric parameter, respectively. δ_Z and η are defined in terms of three principal components (δ_{11}, δ_{22}, and δ_{33}).

$$\begin{aligned}
&\delta_Z = \delta_{11} - \delta_0, \quad \eta = \frac{\delta_{22} - \delta_{33}}{\delta_{11} - \delta_0} \quad \text{when } |\delta_{11} - \delta_0| \geq |\delta_{33} - \delta_0| \\
&\delta_Z = \delta_{33} - \delta_0, \quad \eta = \frac{\delta_{22} - \delta_{11}}{\delta_{33} - \delta_0} \quad \text{when } |\delta_{11} - \delta_0| < |\delta_{33} - \delta_0| \\
&\text{where} \quad \delta_0 = \frac{\delta_{11} + \delta_{22} + \delta_{33}}{3}
\end{aligned} \tag{9}$$

Figure 8 shows the temperature dependence of τ_c determined for dextran methine carbon in freeze-dried dextran and freeze-dried γ-globulin/dextran formulation. For both systems, the τ_c of dextran methine carbon exhibits a significant change in the temperature dependence around the T_{mc} (35°C), the critical temperature of molecular mobility as determined by the spin-spin relaxation of proton. The greater decrease in the τ_c of dextran methine carbon at temperatures above the T_{mc} indicates that the motion of methine groups is significantly enhanced by increased global motion in addition to local segmental

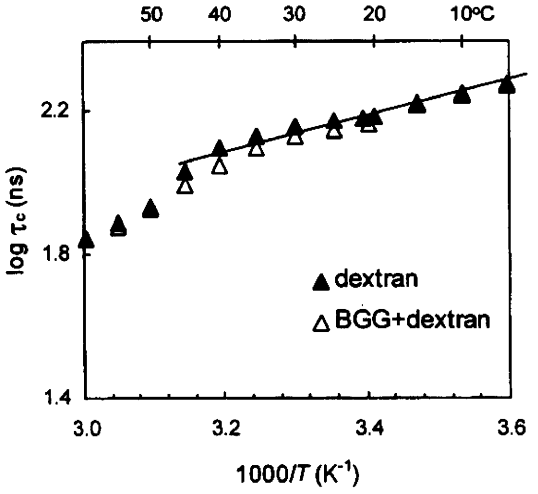

FIGURE 8 Temperature dependence of correlation time for dextran methine carbon in freeze-dried γ-globulin containing dextran 40 kDa.

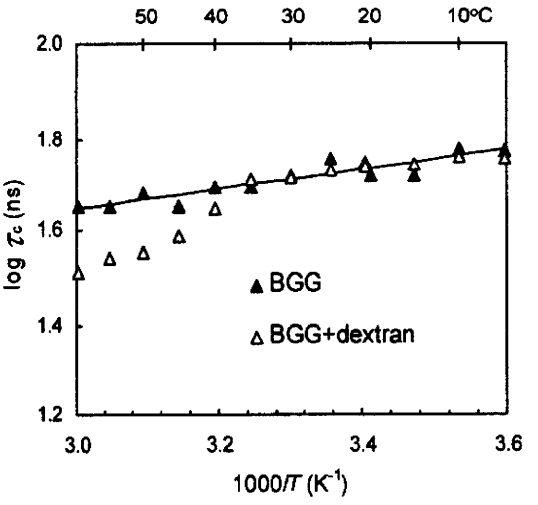

FIGURE 9 Temperature dependence of correlation time for γ-globulin carbonyl carbon in freeze-dried γ-globulin containing dextran 40 kDa.

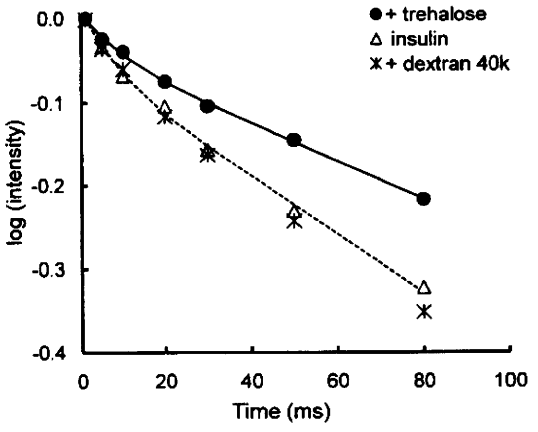

FIGURE 10 Time course of spin-lattice relaxation for insulin carbonyl carbon in freeze-dried insulin, insulin-dextran, and insulin-trehalose systems at 25°C and 12% RH.

motion. This interpretation is supported by the greater decrease in the τ_c of dextran methine proton at temperatures above the T_{mc}, as described in the previous section on proton $T_{1\rho}$ (Fig. 6).

The τ_c of the carbonyl carbon of freeze-dried γ-globulin exhibits linear Arrhenius-like temperature dependence as shown in Figure 9. In contrast, the τ_c of the carbonyl carbon of γ-globulin freeze-dried with dextran exhibits a change in the temperature dependence around 35°C, similar to that observed for the τ_c of dextran methine carbon. This indicates that at temperatures above T_{mc}, the molecular motion of γ-globulin is coupled with that of dextran, even though dextran is well known to cause phase separation with proteins.

Along with the T_1 of carbon, the $T_{1\rho}$ of carbon is useful as a measure of molecular mobility. Figure 10 shows the time courses of spin-lattice relaxation determined for the carbonyl carbon of insulin freeze-dried with dextran or trehalose, compared with that for insulin alone (32). Spin-lattice relaxation is not affected by dextran, but it is significantly retarded by trehalose. The $T_{1\rho}$ of